Light: Science & Applications (2016) 5, e16133; doi:10.1038/lsa.2016.133
© 2016 CIOMP. All rights reserved 2047-7538/16
www.nature.com/lsa

REVIEW

Ultrafast laser processing of materials: from science to industry

Mangirdas Malinauskas[1], Albertas Žukauskas[1], Satoshi Hasegawa[2], Yoshio Hayasaki[2], Vygantas Mizeikis[3], Ričardas Buividas[4] and Saulius Juodkazis[4,5,6]

Processing of materials by ultrashort laser pulses has evolved significantly over the last decade and is starting to reveal its scientific, technological and industrial potential. In ultrafast laser manufacturing, optical energy of tightly focused femtosecond or picosecond laser pulses can be delivered to precisely defined positions in the bulk of materials via two-/multi-photon excitation on a timescale much faster than thermal energy exchange between photoexcited electrons and lattice ions. Control of photoionization and thermal processes with the highest precision, inducing local photomodification in sub-100-nm-sized regions has been achieved. State-of-the-art ultrashort laser processing techniques exploit high 0.1–1 μm spatial resolution and almost unrestricted three-dimensional structuring capability. Adjustable pulse duration, spatiotemporal chirp, phase front tilt and polarization allow control of photomodification via uniquely wide parameter space. Mature opto-electrical/mechanical technologies have enabled laser processing speeds approaching meters-per-second, leading to a fast lab-to-fab transfer. The key aspects and latest achievements are reviewed with an emphasis on the fundamental relation between spatial resolution and total fabrication throughput. Emerging biomedical applications implementing micrometer feature precision over centimeter-scale scaffolds and photonic wire bonding in telecommunications are highlighted.
Light: Science & Applications (2016) **5,** e16133; doi:10.1038/lsa.2016.133; published online 12 August 2016

Keywords: biomedical applications; direct laser writing; functional microdevices; material processing; nonlinear light–matter interaction; 3D structuring; ultrashort laser pulses

UNIQUENESS OF ULTRAFAST LASER PROCESSING

The possibility of three-dimensional (3D) writing in glass[1] and polymers[2] using tightly focused femtosecond (fs) laser pulses, demonstrated roughly two decades ago, has attracted attention in a wide range of areas related to academic research and engineering. The fabrication of 3D objects with a size comparable to that of a living cell and comprising even finer details[3] suggests a realization of remotely controllable 3D micro-bots to perform *in vivo* healing missions or the creation of all-optical information processors integrated on a single 3D microchip and robust non-erasable optical memory structures. Thus began the race towards these and many other attractive goals. At present, most of those goals have yet to be reached; however, the progress achieved in some areas is significant. Currently, optical memories with data density exceeding ~ 1 Tbit cm^{-3} (Refs. 4,5), waveguide-based optical information processing structures[1], elements of optical quantum computing systems[6,7], 3D photonic crystals (PhC)[8] and micro-mechanical/biological systems[9,10] are obtainable using ultrashort laser pulses. Here, we discuss these achievements and outline current trends in the development of laser processing and its applications, which are bound to make ultrashort laser fabrication an indispensable tool for future nanotechnologies.

Unrestricted freeform manufacturing in 3D-space on the mesoscale spanning the critical dimensions of 10 nm to 100 μm in feature sizes has been an engineering curiosity over the last 10–15 years. Endless incarnations of micro-copies from real-world items were fabricated in a variety of photo-polymers, recorded in glasses and crystals. This endeavor pushed and explored the limits of novel 3D fabrication and experimented with optimization for a higher throughput and resolution[11]. The efforts continue to this day and challenge well-established benchmarks in resolution, feature size, precision and efficiency developed over more than 50 years in the microelectronics industry. Comparison of 3D emerging technology with a mature two-dimensional (2D) micro-technology is only partially fair owing to a qualitative difference in the 3D character and the capability of laser manufacturing. Both approaches have fundamental limitations set by the wavelength of fabrication for electrons and photons, respectively. The difference in the relevant wavelengths is revealing: the electron's de Broglie wavelength at a typical $V = 50$ kV acceleration voltage in

[1]Laser Research Centre, Department of Quantum Electronics, Physics Faculty, Vilnius University, Saulėtekio Ave. 10, LT-10223 Vilnius, Lithuania; [2]Center for Optical Research and Education (CORE), Utsunomiya University, 7-1-2 Yoto, Utsunomiya 321-8585, Japan; [3]Research Institute of Electronics, Shizuoka University, 3-5-3-1 Johoku, Naka-ku, Hamamatsu 432-8561, Japan; [4]Centre for Micro-Photonics, Faculty of Science, Engineering and Technology, Swinburne University of Technology, Hawthorn, VIC 3122, Australia; [5]Melbourne Centre for Nanofabrication, ANFF, 151 Wellington Road, Clayton, VIC 3168, Australia and [6]Center of Nanotechnology, King Abdulaziz University, Jeddah 21589, Saudi Arabia
Correspondence: M Malinauskas, Email: mangirdas.malinauskas@ff.vu.lt; S Juodkazis, Email: sjuodkazis@swin.edu.au
Received 7 January 2015; revised 4 March 2016; accepted 9 March 2016; accepted article preview online 14 March 2016

electron beam lithography is $\lambda_e = \frac{h}{mv} = \sqrt{\frac{h^2}{2emV}} \simeq 0.055$ Å (nonrelativistic), where h, e, m are the Plank's constant, electron charge and mass, respectively, whereas the light wavelength $\lambda_l = 5000$ Å (a green color) in 3D-laser writing.

Lasers entered and now dominate the fields of welding, drilling, cladding and manufacturing with a unique capability of 3D robotic light delivery at a 0.1–10 m scale and pointing stability of ~1 mm (for example, in the car manufacturing industry) since circa 1980 (Ref. 12). Lasers operating at 1 or 10 µm wavelengths and at long pulse or continuous-wave (cw) mode are practical and useful, yet unsuitable for fabrication tasks at scales smaller than 1 mm. Thus, they are presently challenged in precision and resolution by reliable ultrashort pulsed lasers. A double innovation in (i) the development of new materials and (ii) laser sources that are better suited for 3D microprinting was required for the continued progress of laser fabrication and the long-praised resolution of fabrication not being the driving factor.

Now, with the emergence of a new generation of reliable fs-lasers, a set of new materials and backing by science of light–matter interaction at the nanoscale with cross-sections smaller than 100 nm, miniaturization of 3D-laser fabrication is advancing and innovating. To demonstrate the versatility and potential of the new technology, 3D inscription, additive manufacturing and surface texturation techniques are shown to reach the high throughput required for industry. A selected few representative examples illustrate the capabilities and truly unique features of fs-laser fabrication.

IS FABRICATION USING ULTRAFAST LASERS A FUTURE TECHNOLOGY?

Industrial challenges

Manufacturing has its own conservative pace of development and justification of new investments. Considerable innovation that brings a new quality to the product simultaneously with higher productivity is always required for the next cycle of technological renovation, which occurs on a 7–10-year-modernization cycle on a factory floor. In manufacturing with lasers, their acquisition and maintenance costs, reliability and longevity were always the main driving forces for industrial installations. The innovation that an ultrashort pulsed laser can bring to manufacturing is discussed next from the perspective of unique control over the light–matter interaction when ultrashort laser pulses are used and in view of the practical requirements of high productivity.

The additive manufacturing, cutting and welding with CO_2, YAG and fiber lasers that operate at 10 or 1 µm wavelengths with a cw or pulsed-mode operation are already powering the automotive, construction and marking industries[12]. The feed speeds of a workpiece are ~10 cm min^{-1} (~1 mm s^{-1} or in specific cases even higher) for marking and welding applications realized with lasers with an average power of ~0.1–1 kW. The target industrial macro-fabrication speed is ~10 cm min^{-1} for a linear scan, including turning points, which can already be demonstrated in fs-laser micro-fabrication[13,14] with a recent record in waveguide writing speed of 200 mm s^{-1} (Ref. 15) on the screen of a mobile phone inside Gorilla glass. Another efficient and confined light delivery is a filament[16] self-formed in water, which can assist in uniform energy delivery along the beam propagation direction[17]. This helps laser fabrication of curved surfaces where tight focusing would require axial position adjustments for precise matching of the focal region and the sample's surface[18]. The principle of this approach is depicted in Figure 1. The formed filament can have a high aspect ratio (length to width) and experimentally realized more than 2 mm in length and just tens of micrometers in diameter[13]. When a laser raster scan or multi-line exposure mode is used for a fill exposure of 3D volume of a workpiece/pattern, the fabrication time quickly increases to hours for an object with 3D cross-sections of ~1 in.

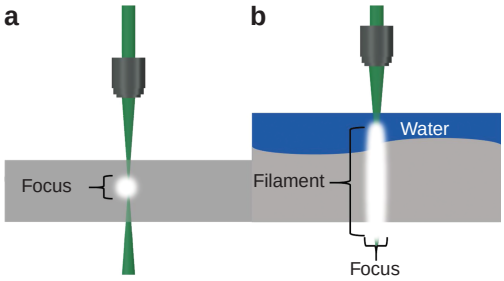


Figure 1 Beam focusing approaches: (**a**) a beam is focused on the surface or volume of a material; (**b**) an fs-beam is focused on liquid and forms a light filament suitable for processing of transparent and opaque workpieces at different axial locations or curvature of the surface. Reproduced with permission from Ref. 13. JLPS. All rights reserved.

The fastest available beam scan approach employs mechanical galvo-scanners that can deflect the beam even faster than 10 m s^{-1}. However, such high-speed scanning is achievable only for linear structures. When turning tight corners, acceleration becomes a serious issue. The acousto-optical device-based deflector enables increased beam scanning velocities up to 2 m s^{-1} with no inherent limitations on a turn radius maintaining high positioning repeatability[19]. In addition, powerful laser sources can be used for parallel multibeam[20] fabrication as well as employing passive[21] or active beam shaping techniques[22]. Such implementations dramatically increase fabrication throughput. Recently, tomographic data were used as a master CAD model for laser 3D fabrication[23], an approach adopted from 3D printing.

Fs-laser fabrication have application where high precision is required, where structuring of the surface and bulk of transparent materials that are brittle and hard must be performed. If composite and layered materials must be structured in a complicated 3D fashion, it can be performed by fs-laser structuring. This has been understood from the basics of light–matter interaction in which pulses shorter than the energy relaxation between electrons and lattice ions can deliver energy with the highest precision and without plasma screening/reflection effects[24–26].

Scaling from 2D to 3D

Because high precision and small feature size are incompatible with large-throughput fabrication—Tennant's law[27]—and by following the universal trend of miniaturization, we expect future applications for fs-laser manufactured structures and objects to be used in smaller-footprint lab-on-a-chip applications. Lab-on-a-chip devices have typical dimensions of 1×1 cm^2 and feature sizes of the functional elements such as channels and optical elements on the order of a cross-section of an optical fiber (a human hair) of ~100 µm. At this already challenging scale, the surface finishing and smallest structures should be controlled at $\lambda/20$ nm precision/resolution for optical functionality.

Fs-laser sources at 50–1000 kHz repetition rates and average power up to 10 W for a typical wavelength $\lambda \simeq 1$ µm and pulse duration $\tau_p \simeq 200$ fs have reached an industrial grade in terms of reliability and capability of fabrication at the required ~10 cm min^{-1} workpiece feed rates. Tennant's law linking the resolution, R (nm) and the

doi:10.1038/lsa.2016.133

throughput, T_{2D} ($\mu m^2\,h^{-1}$) of fabrication via a planar lithography predicts the following scaling[27]:

$$T_{2D} = (R/2.3)^5 \text{ or Resolution} = 2.3\sqrt[5]{\text{Throughput}} \quad (1)$$

Following the arguments of scaling, for a 3D fabrication via lithographic approach, one could expect $T_{3D} = (R/2.3)^{5\times 2/3}$ $\left(\text{or } R = 2.3T_{3D}^{0.3}\right)$ with T_{3D} ($\mu m^3\,h^{-1}$), which follows from area-to-volume scaling. However, Tennant's law is for the 2D fabrication; for the production of 3D objects, we use a more general expression $R = C\times T_{3D}^{0.3}$, where value of $C = 32.2$ is taken to pin the power plot (Figure 2) to the natural throughput of protein production in a 3D conformation by a ribosome; the resolution (often referred to but not to be mixed up with the individual feature size) is taken as 1 nm. This C value corresponds to the production rate of 20 amino acids per second in a cell[30]. It is noteworthy that this comparison of direct writing used in fabrication—for example, building 3D objects by laser polymerization[28] or glass structuring[29]—is valid because ribosome is also constructing 3D proteins from a linear code[30]. Another measure of the 3D production rate can be made from the growth rate of cells. Human nails grow at a 1 nm s^{-1} linear speed, which means 3.6 $\mu m^3\,h^{-1}$, and is similar to the protein production rate.

Figure 2 shows typical Resolution ∝ Throughput regions marked by ovals for the manipulation of single atoms by scanning tunneling microscopy (STM), writing by oxidation of SiO_2 with an atomic force microscope (AFM) needle, standard electron beam (EBL) and optical mask projection lithographies. These are 2D technologies that obey Tennant's scaling $T_{2D} = (R/2.3)^5$, which is a pure empirical dependence. Interestingly, starting from the current 22-nm node of modern complementary metal oxide semiconductor (CMOS) lithography, the field transistor design allows the exertion of 3D control of the depletion regions in the channel. Hence, the future of planar 2D technology tends to become 3D functional as the feature size is reduced[31]. Apparently, for the 3D case (Figure 2), direct laser writing by polymerization[28] and volume Bragg gratings formed by axially extended Bessel–Gauss fs-beam[14] delivers a 3D finished and functional structure. For example, direct laser writing with fs-laser pulses delivers 3D fabrication of $\sim 10^3$ μm^3 s^{-1} with focal spot size $d = 1.22\lambda/NA \simeq \lambda$

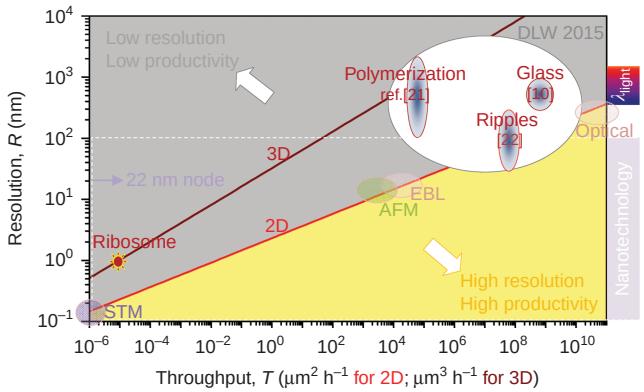


Figure 2 Tennant's scaling: state-of-the-art of nanotechnology in 2003 for the resolution vs. throughput $R = 2.3^5$ T_{2D} (Ref. 27). Direct 3D laser writing for polymerization[28] with $T \simeq 10^9$ μm^3 h^{-1}, Bragg grating recording by Bessel–Gauss fs-beam in glass[14], surface ripple formation on crystals/glasses[29] are marked along with the Tennant's law predictions rescaled for the 3D $C\times 10^6$ μm^3 h^{-1} with $C = 32.2$ taken from the speed of protein production in ribosome[30] (see text for details). The size of elliptical markers is representative of the resolution span; the current 22 nm node of modern CMOS lithography is marked by an arrow.

for 3D structuring of silicone elastomer[28,32]; here, NA is the numerical aperture of the objective lens. On the Resolution ∝ Throughput plot (Figure 2), the corresponding 3D fabrication examples tend to cluster towards the desirable lower-right side of the lines representing Tennant's law for the 3D case. This shows that for 3D-laser fabrication, the throughput can meet industrial standard at the required resolution for 3D manufacturing.

ULTRAFAST LASER LITHOGRAPHY

The trend of miniaturization, which began in CMOS electronics, is currently spreading to other areas, such as micro-optics, micro-fluidics and micro-mechanics. In these fields, new functionalities of micro- and nanostructures stem from physical or chemical responses arising because of size and shape-related effects and, in the case of optical systems, benefit from enhanced interactions between light and matter in artificially structured media. Perhaps the most intuitively appealing examples of such applications are optically controlled mechanical phenomena—for example, laser trapping—which rely on opto-mechanical susceptibility of microscopic particles and structures to optically generated minute forces and torques. Other rapidly evolving areas are optics of plasmonic nanoparticles and PhCs, which enable control over light emission, absorption and propagation at the nanoscale, a demand strongly stimulated by the need for green and sustainable use of energy and materials. Below, we will mainly focus on the structuring of dielectrics and their new optical, mechanical and biomedical functionalities.

Requirements for surface quality

Micro- and nanofabrication of optical structures requires surface roughness $< \lambda/20$, ($\simeq 20-40$ nm for visible wavelengths) to reduce random light scattering. Although this requirement can be in some cases alleviated by post-fabrication treatment—for example, controlled remelting, lapping and polishing of microscale objects—it still remains a difficult task. Therefore, the fabrication techniques capable of directly delivering the required quality are essentially preferred. In this respect, the potential of fs-laser lithography has been demonstrated many times, and some examples will be given in the sections below. In general, the surface quality of laser-fabricated optical elements is high enough to enable their direct use in photonic applications.

Materials and processing techniques

Owing to the requirements of high surface quality and low random scattering, laser fabrication of optical micro- and nanostructures prefers nondestructive photomodification processes over optical breakdown or other destructive processes. Therefore, liquid photo-curable organic resins and negative-tone photoresists are mainly used as initial materials for direct laser writing (DLW) lithography. In these materials, optical absorption induces photochemical reactions, such as photopolymerization (curing). In liquid resins, this process leads to liquid-to-solid transition, whereas in photoresists—which in most cases are exposed as dry, solidified films—photomodification has a latent character. After the laser structuring, unexposed liquid resin is rinsed away, whereas unexposed resist is dissolved in a developer and removed from the structure. Finally, the rinse liquid is dried; this is a critical step for finely patterned, fragile structures, because they may become completely destroyed by powerful capillary forces. These undesired effects can be suppressed by the use of freeze-drying or critical-point drying techniques to eliminate the surface tension effects[33,34].

Historically, liquid resins were the first materials to show potential for 3D-laser structuring[2,35–37], but later negative-tone photoresists became widely used owing to their higher stability during processing and lower post-drying shrinkage. Among photoresists, epoxy-based chemically amplified photoresist SU-8 has acquired wide popularity[8,38–40], because this resist, specifically intended for microfabrication of mechanical components via ultraviolet lithography, was already commercially available during the early steps of development of 3D-laser lithography. SU-8 is optically transparent in visible and infrared (IR) spectral ranges, but can be exposed via two-photon and multi-photon absorption, ensures submicron resolution, has a refractive index ≈1.5, and is mechanically strong and biocompatible. Numerous demonstrations of micro- and nano-photonic structures—for example, 3D PhCs—fabricated in SU-8 can be found in the literature[41,42].

Subsequently, new classes of photoresists specific for laser lithography were developed, aiming to further improve spatial resolution, simplify post-processing and reduce drying-related shrinkage. A class of photoresists based on a zirconium propoxide sol–gel[43] developed by a collaboration of several groups offers significantly improved spatial resolution, low proximity effect (thin threads that evolve randomly and uncontrollably between closely spaced larger features) and low shrinkage[44]. This is achieved by combining organic and inorganic components and various modifications of this hybrid material, also known as SZ2080, which were synthesized to target specific purposes—for example, assisting subsequent metallization by the inclusion of metal-binding moieties[45] and the improvement of spatial resolution by inclusion of mobile quenching molecules[46]. Tuning proportions of photoresist components, such as glass-forming silica, zirconia, titania and methylmetacrylate plastic-like moieties allow a flexible choice of mechanical and optical properties of micro-optical elements[47,48]. In addition to SZ2080, a line of IP resists developed by and available commercially from Nanoscribe GmbH[49] offers similar advantages for ultrafast laser structuring. IP photoresists also include liquid photoresists, which can simultaneously act as an index-matching liquid during the DLW process and has enabled the achievement of structures with extremely large heights[50]. Because swelling and shrinkage during development and drying is inherent to negative-tone photoresists[33,51–53], shrinkage effects can be significantly suppressed by using positive-tone resists borrowed from the semiconductor industry[54,55]; however, in this case, the total exposed (to be removed) volume may increase, and the fabrication time may lengthen somewhat in the case of sequential DLW processes. Photosensitivity of photoresists and resins was conventionally tailored by adding photoinitiators to these materials. Recently, careful control over spectral and temporal characteristics of fs-laser pulses has enabled precise control over photo-excitation via multi-photon and avalanche ionization as well as by controlling the thermal conditions at the focal volume inside a pure resist. A combination of high pre-breakdown irradiance and fast scanning opens the possibility to tame chemical-free radical creation and their thermal cross-linking without the necessity of a photoinitiator[11,56]. Coincidentally, initiator-free cross-linking in silicone[28] has produced biocompatible material free of the bio-toxic cyclic compounds present in most photoinitiators. Strongly 3D-localized thermal curing of resists[57,58] can now be widely explored for microfabrication owing to their fast scan capabilities.

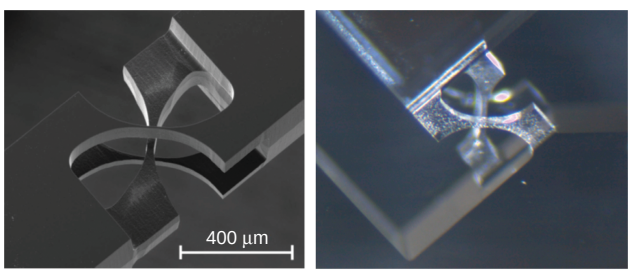


Figure 3 A cross-pivot hinge out of fused silica as a part of a mechanical structure. The images show the three crossed beams and the rounded corners at the location where the beams are connected to the main body. Note the high aspect ratio of the micromachining process. Reproduced with permission from Ref. 76. MDPI. All rights reserved.

With regard to fabrication techniques, the two main methods are holographic fabrication[20–22] and DLW[59–64]. Holographic fabrication exploits nondestructive exposure of a material to a periodic interference field of several coherent laser pulses, and can be implemented using a simple opto-mechanical setup and a wide variety of amplified and unamplified laser sources. Various implementations of DLW are described in the available literature[11,65–67], and DLW setups are commercially available from several companies[49,68–70]. Among the current developments in the practical implementation of the DLW technique is a significant increase of the laser beam scan speed in the sample from ~100 μm s^{-1} toward meters-per-second achieved via the combined use of fast mechanics for sample translation and scanning of the beam focus inside the sample[9,71,72]. Special exposure schemes tailored to improve the axial resolution of DLW can also be added[73–75]. For exposure of photoresist or resin samples, fs-laser oscillators (for example, Ti:sapphire or fiber laser systems) provide sufficient exposure levels. The wide availability and constantly decreasing size and price of these laser sources contribute to the practical applicability of the DLW technique. For exploitation of the DLW technique near or above the laser-induced breakdown threshold in solid crystals or glasses (for example, for waveguide writing and creation of new materials), amplified laser systems providing pulse energies >1 μJ are required.

Next to lithography, the fs-laser irradiation can be very similarly applied for processing of fused silica (the amorphous form of SiO_2) and introduces a novel technology platform for highly integrated all-optical microsystems. In contrast with common approaches that rely on combining materials to achieve particular functions, fs-laser-fabricated microsystems rely on single material monolith, whose properties are locally and 3D functionalized by selective exposure. The combination of functionalized zones with different physical properties allows integration of systems without the need for further assembly of packaging steps or without the need for multiple processing steps, like for instance sequences of layers deposition, exposure and etching steps (Figure 3; Ref. 76). Lastly, there is numerous other additive (and subtractive) manufacturing approaches where ultrashort pulses have significant advantages over longer pulses. To mention a few techniques like laser-induced forward transfer (LIFT) or an intense field-induced self assembly are not reviewed here; see Refs. 77, 78 for the detailed account.

3D micro-optical elements

Aspherical and axicon micro-lenses as well as diffractive optical elements were DLW fabricated directly on the core of the optical fiber[79–81], illustrating the potential of the technique to integrate various components. Figure 4 shows an example of such optical elements fabricated in photoresist SZ2080. Spiral waveplates[59,82] for optical vortex generation (Figure 5) and hybrid refractive-diffractive elements blending diffraction gratings and lenses can be made[83].

doi:10.1038/lsa.2016.133

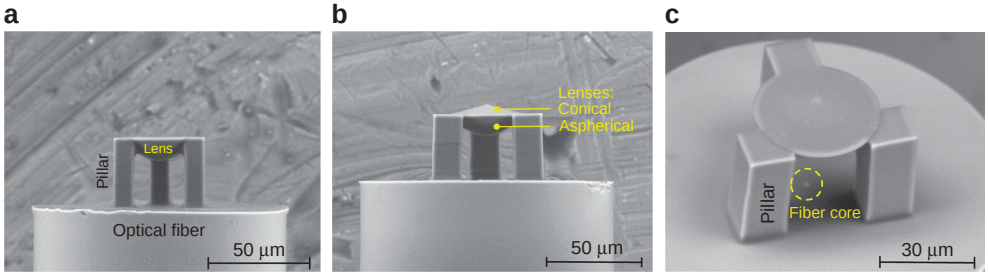


Figure 4 Freeform 3D micro-optical elements fabricated by DLW: hybrid optical elements—aspheric and axicon lenses on a tip of optical fiber. Reproduced with permission from Ref. 81. JLPS. All rights reserved.

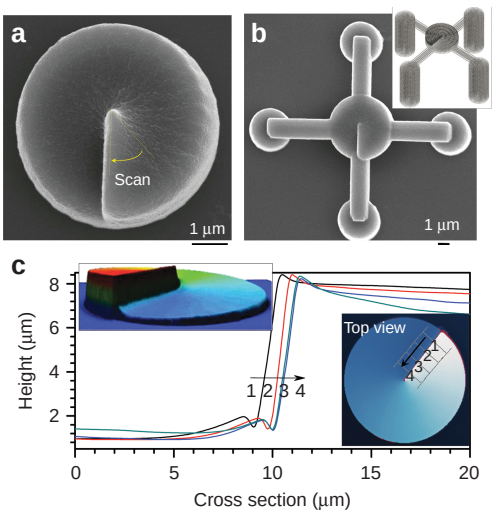


Figure 5 Optical vortex generating spiral waveplates. Smaller (**a**, **b**) and larger (**c**) cross-sections optical vortex generators. (**a**, **b**) SEM images of micro-plates made by point-by-point exposure (inset in **b** shows 3D construction of irradiation matrix). (**c**) Height scans at four locations of the step edge of the spiral plate; diameter of the plate was 60 µm. Reproduced with permission from Ref. 59. Copyright (2010), AIP Publishing LLC.

A rapidly growing field of singular optics exploring the generation and control of optical vortices at a microscale benefits from DLW via polymerization owing to a simple method to achieve ~100% efficiency of the optical vortex generation. Alternatively, planar patterns for the vortex generation—*q*-plates—are made of azimuthally patterned form birefringence inside glass by fs-laser structuring[84,85]; however, they suffer from scattering losses.

It is helpful to stress here that these structures clearly satisfy the high surface quality requirements outlined in the section above and are directly usable. It has been already proved by several studies that there is no shape limitation or restriction of a single element in an array of micro-lenses[86–88]. Obviously, surface quality and optical characteristics of these elements can be retained during their replication—for example by nanoimprint, hot embossing and molding—directly or via an Ni-shim replication[89,90]. Recently, integration of 2D and 3D optical components comprising both passive and active functionalities —namely, a rectangular waveguide of rectangular cross-section that can be $\pi/2$-twisted to form an arch on the substrate—was demonstrated[91]. Thus, the application of ultrashort laser processing can lead to realization of new optical integrated devices with novel functionalities such as optofluidic single-cell counters[10]. Interestingly, by applying different exposure doses, one can achieve 3D or 2D varying material properties, thus producing monolithic components with composite properties[92]. This seems to be an attractive option for producing custom-made freeform gradient refractive index micro-optical elements[93].

One of the primary application areas of ultrafast laser lithography in photoresists and resins has been the fabrication of PhC structures[94–101], especially 3D ones that are difficult or impossible to realize by other available techniques. 3D PhCs with woodpile[41,102], spiral[103,104], slanted-pore[105] and other architectures[64,106] with high optical quality were demonstrated during the last decade. Figure 6 summarizes the structural and optical properties of a 3D woodpile architecture PhC fabricated in SZ2080 photoresist by DLW and dried in supercritical CO_2. Scanning electron microscopy (SEM) images shown in Figure 6 (a) demonstrate the DLW fabrication of highly resolved features, evident from woodpile rods with lateral thickness of $\sim a_{xy} = 135$ nm. The in-plane lattice period (distance between two neighboring woodpile rods), designed to be 1000 nm, is in reality reduced to 940 nm owing to shrinkage of ~ 5% of the PhC lattice. Shrinkage by a similar amount is also evident in the large-scale SEM image in Figure 6(a). The distance between the neighboring woodpile planes is designed to be $a_z = \sqrt{(2)}/4a_{xy}$ to maintain a face-centered cubic (fcc) lattice symmetry.

PhC structures with similar parameters were unexpectedly found to exhibit strong resonant reflection at visible wavelengths, although neither fundamental nor higher-order photonic stopgaps (PSG) are expected to open in this spectral range owing to a fairly large PhC lattice period. Figure 6(b) shows optical image of several fcc woodpile structures similar to that in Figure 6(a), having lattice periods a_{xy} varying in small steps and fabricated at different average powers of the writing laser beam. Observation in reflection mode within an angular incidence range of ±17° clearly reveals the structural color of the PhC structures. The color exhibits redshift with increasing lattice period and writing laser power (that is, dielectric filling ratio) in qualitative agreement with Maxwell's scaling behavior[107], thus indicating that its origin is linked to the periodicity of the PhC. Figure 6(c) summarizes the interpretation of the structural color by comparing the experimental reflectivity spectrum of the PhC structure in Figure 6(a) with the reflectivity spectrum and photonic band diagram simulated using the finite-difference time-domain technique. As can be seen, a fundamental PSG opens along the observation (woodpile layer stacking) direction near the 1400 nm wavelength in the only PSG and results in a near-IR reflectivity band, whereas the visible reflectivity band occurring near the 700 nm wavelength spectrally overlaps with nearly horizontal segments of some high-photonic bands characterized by low group velocity.

Accordingly, resonant backscattering should be associated with coupling losses between incident plane waves and slow-light modes inside the PhC[107]. Exploitation of high-photonic band dispersion

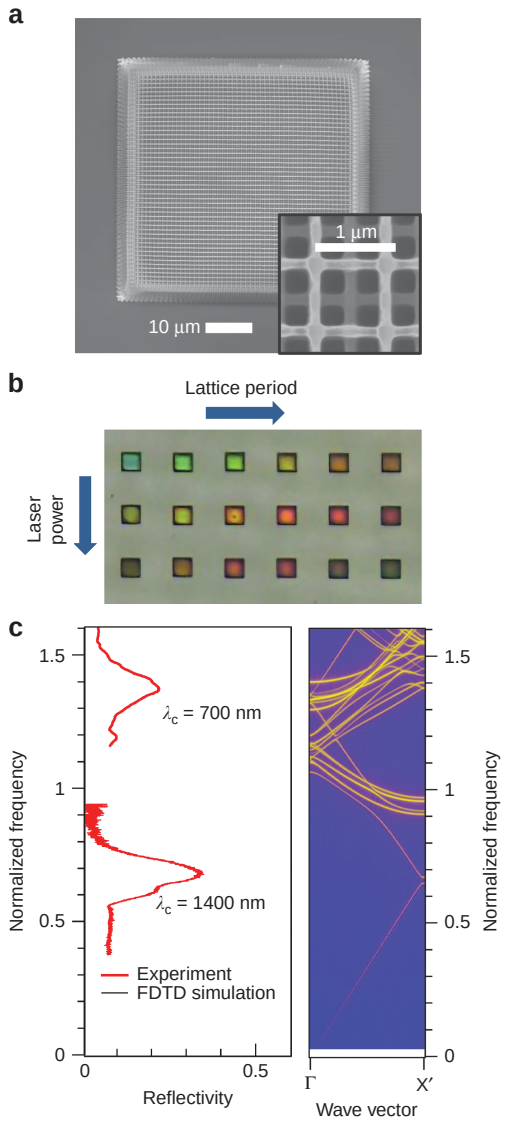


Figure 6 Coloration via slowing light. (**a**) SEM image of 3D woodpile architecture PhC in photoresist SZ2080, (**b**) optical microscopy image of several woodpile structures having different lattice parameters and exhibiting different structural color, (**c**) comparison between experimental optical reflectivity spectrum of the sample shown in **a** and numerically simulated reflectivity spectrum as well as photonic band diagram. Reproduced with permission from Ref. 94. JLPS. All rights reserved.

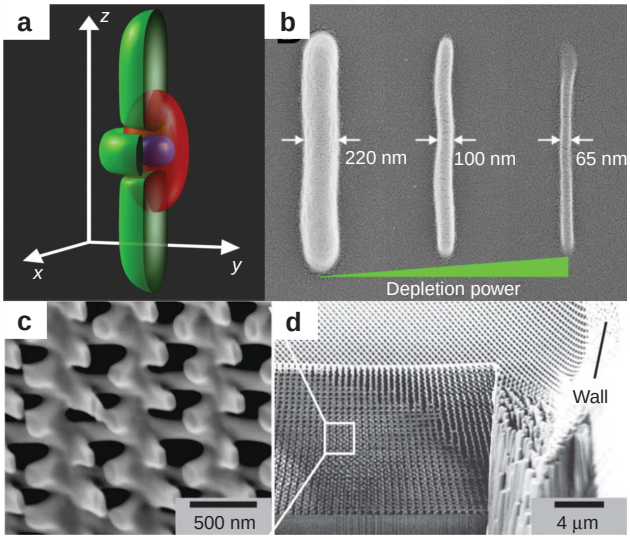


Figure 7 (**a**) A typical DLW STED exposure profile: red volume represents standard focusing exciting the material; green represents a phase mask-generated depletion (bottle beam); violet is the resulting modified volume (excitation is minimized by cutting the side and top-bottom lobes with a shaped depletion beam)[73]. (**b**) Using the same excitation conditions but increasing the depletion power, the feature size shrinks (from left to right, it is minimized from 220 nm down to 65 nm)[73]. (**c**, **d**) Magnified and full-scale image of 3D chiral polarizer structure fabricated employing simultaneous combination of dip-in[50] and STED techniques[111]. Reproduced with permission from Refs. 73, 111. OSA. All rights reserved.

allows realization of PhC-based structural color materials without the need to downscale their lattice period. Slow-light regions are promising for sensors owing to their increased light–matter interaction.

Ultimate feature size vs. resolution

The latest advances in nonlinear polymerization-based laser structuring reveal that it is not the exposure conditions but the reacting material itself that is a real limiting factor for the ultimate resolution[108]. First, one should clearly distinguish the difference between the feature size and the resolution—in other words, dimensions of a single feature and resolved separate features[109]. Although nonlinear light-matter interaction-induced modification volume can be squeezed down to tens of nanometers by reducing the applied laser intensity (the exposure dose), it is not very helpful for ensuring scale-down of the resolution[110,111]. The fabricated structure is revealed by using wet development; the tiny volumes of cross-linked material tend to shrink and become even smaller. Hence, this minimizes the polymerized feature size but hardly improves the resolution.

The stimulated emission depletion (STED) technique, well established in multi-photon microscopy[112], can be implemented to improve both the features size and the resolution, as shown in Figure 7a and 7b. STED-inspired lithography relies on simultaneous photo-induced activation and deactivation of the polymerization process.

The ultrafast excitation pulse drives the photoinitiator molecules to a long-lived intermediate state that initiates polymerization on a relatively slow timescale. A second laser is employed to quench this intermediate to the ground state, preventing polymerization. By spatial beam shaping, the photomodification can be confined to a well-sub-diffraction-limited small region. This research vector was extensively studied by several research groups; M. Wegener's and T. Klar's are among the most active. Their results proved that the feature size can be more confined by optimizing the material for that purpose and applying a dual exposure: an ultrafast excitation and inhibition[113]. Experimentally realized arrangements including phase masks for specific beam shaping are already described in detail elsewhere[111,114]. Most importantly, it was shown that this approach empowers dramatic improvement of not only the lateral but also the axial resolution[115]. This progress makes the DLW lithography technique even more attractive and versatile for the manufacturing of state-of-the-art photonic as well as biological components[116]. Despite these achievements, the topic of achievable resolution and feature size remains actively debated with the main arguments focused on the mechanisms of polymerization and its kinetics[117–120].

doi:10.1038/lsa.2016.133

VOLUMETRIC STRUCTURING OF DIELECTRICS

The unique 3D capability of fs-laser writing is overviewed next for the creation of new materials and strategic fields of telecommunications[121,122] and various biomedical applications[22,23,71,72].

Creation of new materials via extreme pressure and temperature conditions

With tight focusing and concentration of light into a small submicron focal spot and by using ultrashort laser pulses $\tau_p \simeq 100$ fs, the intensity reaches several terawatts per square centimeter for small-energy $E_p \simeq 100$ nJ pulses. For such pulses, self-focusing can be avoided because the pulse power $E_p/\tau_p \leq 1$ MW/pulse is below the self-focusing threshold inside the dielectric and semiconductor materials; however, the intensity can already surpass the dielectric breakdown threshold.

In multiple ionized plasma and under strongly nonlinear dynamics of electrons and ions in abrupt pressure and temperature gradients, separation of the ions of different masses occurs[123,124]. After the microexplosion, strong thermal quenching facilitates the recovery of metastable phases of materials. Some of those phases are high-pressure and temperature nanomaterials previously only predicted by modeling. The creation of molecular oxygen in glasses[125]; change of the ionic makeover of complex compounds such as one of the Earth's most abundant minerals, olivine[126]; fixation of highly unstable amorphous phase of sapphire[127]; and formation and recovery of body-centered cubic-Al inside sapphire, which requires pressures such as in the Earth's center[128], are recent illustrative examples.

When a light pulse is squeezed to tens of fs and focused into volumes with cross-sections of sub-wavelength dimensions (hundreds of nanometers) and absorbed at an even smaller volume where dielectric breakdown is created, the energy density reaches levels encountered in the strongest military macro-explosions. A phenomenal scale span over which a hydrodynamical stage of the explosion can be modeled is shown at energies 10^{21} times lower, and time scales are reduced by a factor of 10^7, creating the same Energy/Volume density[129]. At such exotic p, T conditions, defects inside glasses and crystals can be easily created at large densities[5,130–132]. Such strongly altered regions have different chemical etchability in acidic[133,134] and basic[135] solutions now widely used for micro-fluidics, structural analysis of the micro-/nanostructure of the interaction volume and fabrication of 3D micro-parts in silica and sapphire.

Temporal and spatial chirp control allows additional tunability of light–matter interaction of focused ultrashort laser pulses[136–139]. Interestingly, a new metal welding technology based on a spark discharge uses an fs-laser-guide for pointing and chirp control of ionization. This is an example of an industrial process in which subtle parameters of fs-laser pulses are at work. Welding of previously incompatible materials, glasses, ceramics and metals with very different thermal expansion coefficients becomes possible using ultrafast lasers[140,141].

The generation of a white light continuum using fs-laser pulses in water has proved to result in size homogenization of colloidal nanoparticles made by ablation in water[142]. For example, such colloidal suspensions of Au nanoparticles are stable in time against precipitation without surfactant additives and finds increasing popularity in biomedical sensing because of the pure Au surface accessible for functionalization[143].

Passive and active waveguides

Waveguiding regions can be made by direct laser writing inside transparent materials. The guiding occurs in the augmented refractive index locations $n = n_0 + |\Delta n|$, which can be created by stress-induced modifications, defects or densification; n_0 is an unperturbed refractive index of the medium. A fast thermal quenching important for the waveguide recording can be exploited in fs-laser writing. Glass structures typical for the elevated temperatures can be frozen along the written track. A so-called fictive temperature of glass corresponds to the particular glass morphology. In some glasses such as silica, the anomalous behavior is observed when denser phase corresponds to the higher temperature. For silica, the largest refractive index (a mass density) is at $T_{dense} = 1500$ °C[125]. If waveguide writing conditions are chosen such that the recorded track has a fictive temperature close to T_{dense}, a waveguide can be formed by fast quenching. Moreover, the waveguiding region does not exert compressive stress to surrounding regions as in most glasses and crystalline materials where the recorded track is expanded and is not waveguiding. The lowest loss waveguiding has been demonstrated in a tempered Gorilla glass[15]. In crystals, formation of strongly localized stress allows birefringence to be engineered[144] into patterns that can efficiently guide light[145].

Waveguides written by fs-laser processing performs interferometry and quantum computing and is integrated into microfluidic chips[7]. Chip-integrated optical lanterns fabricated by fs-DLW are demonstrated for transfer of the focal plane image of large optical instruments such as telescopes onto CCD or spectrometer slits with preservation of phase information[146,147] with spectral filtering capability via laser-written Bragg gratings[148,149]. This is achieved via a calculation of the 3D trajectory of the waveguide, which maintains the same length and does not approach other waveguides to avoid crosstalk. To maintain coherence from the image plane to the detector array, single-mode waveguides are fabricated. This newly emerging field is branded as astrophotonics[150]. Active laser-written waveguides have been demonstrated at exotic wavelengths and in a small-footprint glass pieces[151] for future on-chip and lab-in-fiber integration[152].

One of the most recent and promising practical advances of 3D-laser writing is emerging in the field of photonic wire bonding (PWB)[122] illustrated in Figure 8. This approach solves issues regarding the connection of silicon photonic circuits made on semiconductor-on-insulator (SOI) industrial platforms to multicore fibers or lasers by DLW 3D lithography and offers novel concept solutions applicable to chip-scale interconnection. Altogether, this induces a dramatic increase of possibilities for the continuously growing telecommunication industry[153]. Here, 3D-laser-written waveguiding structures can be seen to be serving as wires in former microelectronic circuitry, a very logical step when circuits become photonic instead of electrical.

TOWARDS PRINTING BIO-PARTS AND SMART IMPLANTS

The 3D printing of bio-parts[154], food and even houses is a fiction quickly becoming a reality. The principles of stereolithography (3D fabrication) with light scanned over an absorbing surface of resin that is refreshed constantly as the workpiece is moved in the liquid are now taken forward and cross-pollinated with ideas of jet printing and silkography mastered in the solar cell industry. For the mass production of items larger than 1 mm, those new technologies are presenting what could be considered a disruptive technology[155]; that is, they are very simple with a setup acquisition and maintenance cost up to two orders of magnitude smaller than fs-laser-based tools. Indeed, simple light sources or thermally controlled extrusion through a nozzle with a diameter of tens of micrometers is already delivering fascinating 3D fabrication of biodegradable tissue scaffolds and can prototype larger workpieces[156]—for example, benchtop optic holders. In Figure 2, this would correspond to 100 μm resolution and high

productivity $\sim 10^{12}$ μm^3 h^{-1} near the line corresponding to the 3D scaling by Tennant's law.

Figure 9 illustrates the versatility of DLW and the compatibility of different materials that can be combined, exposed and developed for the final 3D complex scaffolds. All materials are transparent with slightly different refractive indexes, helping with the recognition of the earlier fabricated regions in such multiplexed patterns. The control of surface chemistry, wettability and mechanical properties on the mesoscale (from tens of nanometers to tens of micrometers) is currently an active field of research for bio-scaffolds[154,157,158]. DLW control of the volume fraction of a polymer in a 3D structure not only changes its permeability but also provides a method to deliver matching mechanical strength of implant and tissue via fracture toughness engineering[159].

Despite strong competition in 3D fabrication among the different approaches discussed above, a high-precision laser structure will have unique advantages for high-precision scaffold formation where different materials must be combined (Figure 9) or high-resolution

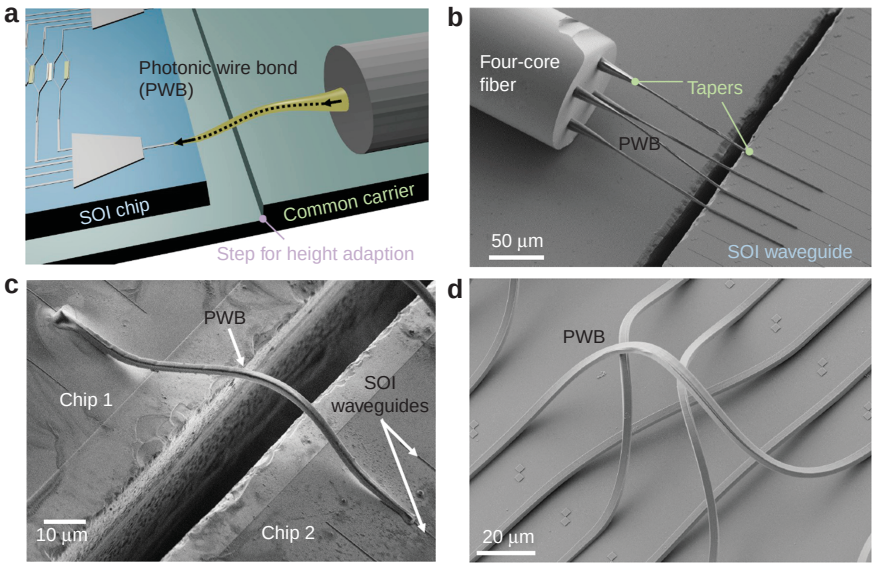


Figure 8 PWB by the 3D DLW lithography approach[121,122]. (**a**) A principal scheme of the PWB enabling connection of an SOI chip with an optical fiber. (**b**) A four-core optical fiber coupled with SOI waveguides by tapered photonic wires. (**c**) An integrated chip with two SOI waveguides coupled together via freeform PWB; note a spatial (lateral) displacement of the SOI waveguides on the separate chips. (**d**) An example of 3D PWB capability enabling virtually direct signal transferring through different communication platforms. Images courtesy of Prof. C. Koos. (2015) IEEE. Reprinted, with permission, from Ref. 122.

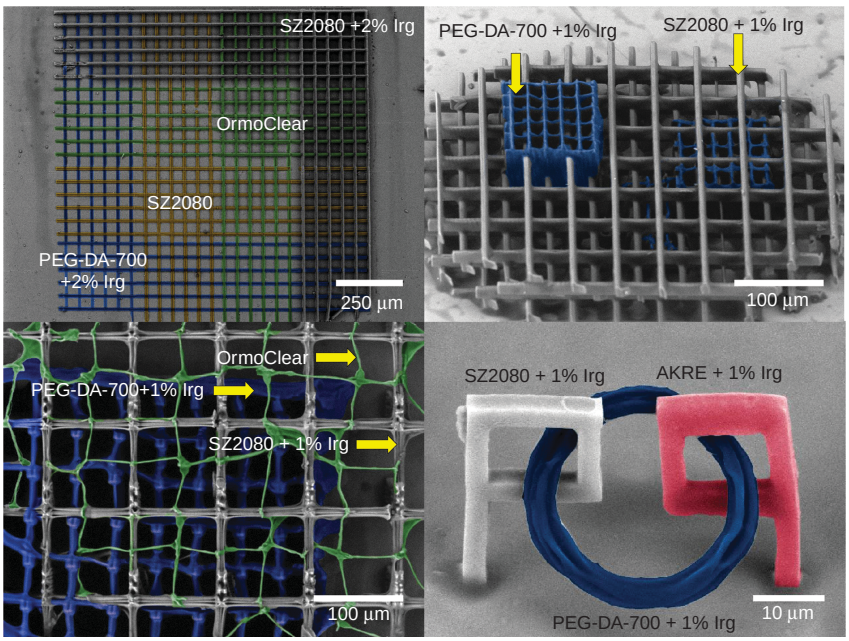


Figure 9 Hybridization of scaffolds made out of different negative-tone photoresists (color-coded for clarity): AKRE—red, SZ2080—gray, PEG-DA-700—blue, Ormoclear—green. Reproduced with permission from Ref. 18. JLPS. All rights reserved.

doi:10.1038/lsa.2016.133

feature size patterns[160,161] are required. Functioning of the cell membrane receptors for opening drug delivery pathways occurs via 3D morphological changes on the membrane on the scale of tens of nanometers[162]. Currently, this is the resolution achievable by DLW lithography in 3D[40] and can be combined with standard nanotechnology methods. Bio-related research for understanding fundamental mechanisms on the sub-cellular level will require the highest resolution of laser writing.

On a larger than cellular scale, the biomedical field is actively researching facile methods for fabrication of macro-3D scaffolds (Figure 10). Recently, a preclinical study of 3D artificial micro-structured scaffolds out of hybrid material SZ2080 fabricated using the DLW technique was reported[154]. The created centimeter-scale membrane constructs were tested both *in vitro* by pre-growing isolated allogeneic rabbit chondrocytes and *in vivo* by implantation into rabbit organisms for up to 6 months (followed by *ex vivo* characterization) (Figure 11). Using a surgical drill, 54 bilateral osteochondral defects with a 3 mm diameter were created. Weight-bearing areas of medial femoral condyles were chosen for a preclinical study. *Ex vivo* histological examination shows that specific 3D pore geometry and pre-growth of chondrocytes before implantation significantly improved the performance of the manufactured scaffolds. The achieved biocompatibility was comparable to collagen membranes widely used in surgery. A successful outcome of the study supports the idea to implement DLW into clinical practice for fabricating patient-specific 3D micro-structured scaffolds that, in combination with cell seeding, may be a significant advance in cartilage tissue regeneration.

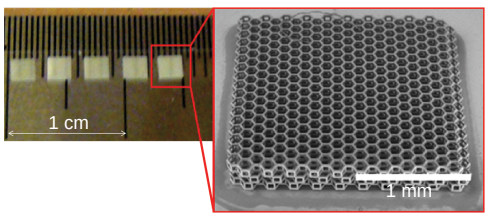


Figure 10 Free (not attached to substrate) macro-3D scaffolds out of SZ2080. Fabrication time 2.5 h/piece with 515 nm/300 fs direct write at 7 mm s^{-1} sample translation synchronized with beam scanning[154].

In addition, it can serve as a tool for generating prototype scaffolds of bio-inspired microarchitectures, and their characterization of mechanical properties required for both hard (bone and cartilage) and soft (muscle, skin, etc.) tissue engineering[163]. Recent studies show that by employing the fs-DLW technique, biocompatible and biodegradable materials such as silk can be 3D structured[164].

Printing via LIFT has already been advanced as a technological solution for the fabrication of microelectronic circuitry[165], and is applicable for the transfer of biomaterials with low damage when ultrashort laser pulses are used. The printing tape principle is applied to form light-absorbing film with functional materials facing the substrate onto which it will be transferred. When ultrashort laser pulses are used, the transfer gaps can be larger, and more directional LIFT is performed owing to the efficient and spatially well-controlled energy deposition[166].

Apart from 3D printing by laser-assisted processing and LIFT, ultrashort laser applications in surgery is another vast field with huge potential. Very precise energy delivery in eye surgery[167] and focusing through a turbid medium using spatiotemporal focusing[168] are just a few examples in which unique control over the delivery of ultrashort laser pulses to the modification/surgery point can be exercised.

Direct write additive manufacturing processes are unique in flexibility yet inherit the underlying limitation of being time consuming owing to the serial nature of point-by-point structuring[169]. The current development of fs-pulsed industrial high-repetition-rate lasers limits the DLW technique by either an efficient sample positioning or beam scanning for high-throughput manufacturing. Recently, a continuous generation of monolithic polymeric parts was demonstrated using stereolithography-based 3D printing, which is believed to allow print manufacturing of parts in minutes instead of hours[170]. The control of the polymerization mechanism using an oxygen-permeable membrane is responsible for faster 3D printing by up to two orders of magnitude.

COMPLEX LIGHT FIELDS

Experimental studies have shown that complex 3D microstructures can be polymerized by multiple foci created and translated by a holographic spatial light modulator (SLM)[171] and can be exploited up to the diffraction-limited spatial resolution[172]. This enables efficient

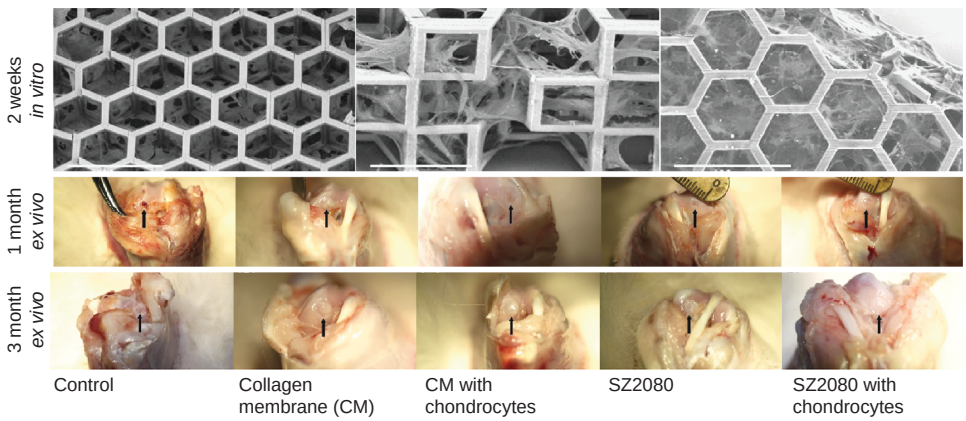


Figure 11 First *in vivo* tests of laser-fabricated scaffold[154]. SEM images of a segment of centimeter-scale membrane tested *in vitro* by pre-growing isolated allogeneic rabbit chondrocytes for 2 weeks; scale bar 100 μm. *Ex vivo* photo images after implantation of laser-fabricated 3D scaffold pre-incubated with chondrocytes and implanted into rabbit's knee (marked by arrow) after 1 and 3 months; 54 bilateral osteochondral defects 3 mm in diameter were created using a surgical drill at the weight-bearing areas. Reproduced with permission from Ref. 154. IOP. All rights reserved.

generation of up to 10 independent foci for parallel holographic fs DLW. Currently, a common SLM ensures a 60 Hz refresh rate, but it can be further increased by the application of faster modulators that are commercially available (200 Hz) with even higher rates expected in the near future[173].

When SLM is too slow for an application, an optical element can be made for a specific phase pattern required for laser fabrication. Recently, for material processing using fs Airy beams, such an optical element was made in glass by a form-birefringent pattern[174]. Airy beams are advantageous for glass scribing, cutting and complex edge and corner formation on a workpiece. With the Airy beam scribing and glass-breaking, a spontaneous self-detachment of a fiber-like structure was induced, offering an alternative way to fabricate glass cantilevers[174].

Development of beam shaping is leading to solutions in which simultaneous control of timing, positioning, phase and polarization of the one or several laser pulses is performed. Surface or bulk modification of transparent materials becomes less distinct in the case of high-intensity ultrashort laser pulses. High intensity can be created inside the material at its optical transparency window as well as in subsurface regions. By creating a high-density electronic excitation, a newly introduced interface then acts as a transient meta-surface that responds to different parameters of the incoming light: polarization, spatial and temporal chirp, ponderomotive action at high intensity and angular momentum of the beam.

Nanotexturing by polarization control

In many cases, it is already proven that peak intensity is a more important parameter than the total energy dose for the required modification. The influence of other parameters, however, can also be very important—for example, the polarization is actively studied in control of ablation and formation of (nano-)ripples.

The structuring of materials by ultrashort laser pulses demonstrated new morphologies in nanotexturing of the surface and volume by self-organized quasi-periodic structures—ripples[29,84,175,176]. Photo-excitation of electron-hole solid-state as well as breakdown plasmas are leading to the formation of sub-wavelength period ripples via imprint of a surface wave on the substrate–plasma interface. A surface wave on a plasma is created when the real part of dielectric permittivity $\mathbb{R}\varepsilon^* < -n^2$, where n is the refractive index of the dielectric medium and a phase matching between the surface wave and the **k**-vector of photons is met. Because the TM-mode with E-field polarized in the plane of incidence (p-polarization) is the most efficient in launching the surface wave, most of the observed ripples on the surface have an orientation perpendicular to the E-field (or a wave vector **k** of the ripple-grating is parallel to **E**). Hence, polarization becomes one of the key control parameters for surface and in-volume formation of ripples, which is shown next for the case of arbitrary and simultaneous control of several beamlets.

Dynamic real-time beam shaping

The polarization and wave front tilt control provides a way to manipulate surface nanotexturing and ripple formation. Figure 12 shows a method to prepare arbitrary polarization, including vectorial beams using SLMs and polarizing optics: $\lambda/4$ and $\lambda/2$ quarter- and half-waveplates QWP and HWP, respectively[169]. The polarization of the output beam $\mathbf{E}_{out}$ is given:

$$\mathbf{E}_{out} = Q_{\frac{\pi}{4}} S_{\beta} H_{\frac{\pi}{8}} S_{\alpha} \mathbf{E}_{in} \equiv \frac{e^{i\alpha}}{2} \begin{pmatrix} -i\cos\beta + \sin\beta + 1 \\ -\cos\beta - i\sin\beta + i \end{pmatrix} \quad (2)$$

where $\mathbf{E}_{in}$ is the Jones vector of the linearly polarized input beam, the subscripts H and Q are the azimuthal angles of the respective HWP and QWP plates, and α, β are the phase retardation applied to the pair of SLMs, respectively. The wave front and polarization of the output beam are independently controlled by choosing α and β. For 3D fabrication, SLMs[74,177] are also useful for compensation of aberrations—in particular, spherical—due to a refractive index mismatch between the substrate and the workpiece and a different depth of focus[178]. Airy beams[179] can be made using SLMs and are very promising in laser cutting applications similarly to the Bessel–Gauss beams[180].

Different incarnations of polarization and phase control setups using SLMs, diffractive optical elements and axicon lenses can be used to generate light intensity distributions, such as doughnut, Gaussian–Bessel[181,182] or flat-top. Experimenting with such beams is a currently active field of investigation along with the control of spatial-temporal focusing[168]. Arrays of beams with individual control of polarization, intensity profile and front tilt can speed

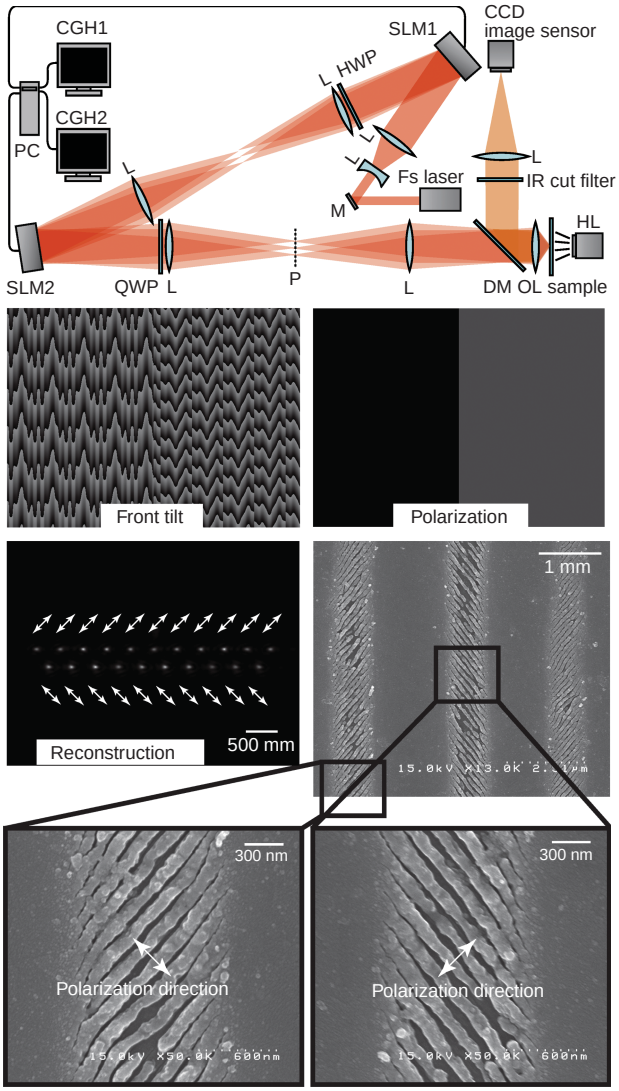


Figure 12 Optical setup with two SLMs for independent control of the wave front tilt and polarization. HWP, QWP and SLM phase masks allows an arbitrary control of the polarization and wave front tilt. SEM images of the single-pass scan ablation of indium tin oxide with adjacent lines polarized differently. Reproduced with permission from Ref. 169. Taylor & Francis Ltd, http://www.tandfonline.com. All rights reserved.

doi:10.1038/lsa.2016.133

up fabrication and more efficiently use laser power in industrial applications[183].

CONCLUSIONS AND OUTLOOK

This mini-review of the state of the art and emerging applications shows the maturity of the ~20-year-old field. The productivity of fs-laser fabrication required for practical applications is demonstrated to be consistent with technologically matured fabrication methods used in 2D planar microelectronics and is now challenging true 3D microfabrication. A comparison with the production of basic 3D building blocks in a living cell—proteins—that acquire 3D conformation encoded in a linear RNA or DNA sequence is shown to follow similar scaling to the fastest examples of direct laser writing used for fabrication of fully functional 3D patterns: optical gratings, bio-scaffolds and PhCs. The 3D wiring of future telecommunication circuitry by 3D waveguides is another successful emerging application.

Biomedical applications involving phenomena from the receptor scale of ~10 nm up to implantable 3D scaffolds with cross-sections >1 cm require adequate biocompatible materials and processing approaches to structure them. Here, we show that modern laser processing with ultrashort laser pulses can address this challenge from the resolution, productivity and materials points of view. By controlled laser curing, photoinitiators become obsolete[56], and light–matter interaction is controlled solely by parameters of light. This feature opens the window to the use of tested biocompatible materials without bio-toxic additives and polymerization promoters[28]. In the future, proteins can be used for optical applications and laser structured from micro- to macroscale patterns or devices[184].

Advances in the understanding of light–matter interaction peculiarities in different materials at diverse conditions of ultrashort pulse delivery onto the surface or inside transparent materials are helping simplify material processing protocols. The reliability of lasers and maturity of fs-pulse control in terms of duration, spatiotemporal chirp and focusing, and polarization meets the 24/7 requirements of industrial applications. Time will tell the extent to which these methods will become niche for this technology in real-world applications within the next few years. Rival technologies based on long pulses and continuous laser radiation along with fast and precise workpiece positioning and 3D printing are 'disruptive technologies'[155]. Innovative disruptive technologies have proved in the past to be commercially successful. Could the demonstrated fabrication at the feature size of ~100 nm and submicron spatial resolution (a separation between individual features) delivered at the millimeter scale be a 'tipping point'[185] for industrial adaptation of fs-laser fabrication? The millimeter-size 3D scaffolds can be made out of the same material and laser cured without toxic initiators for implant applications within a practical time frame. This span of mesoscales from the formation of nano-features to implantable structures is a unique and appealing characteristic of 3D printing by DLW. The Tennant scaling law shows that this 3D technology is mature in terms of its industrial productivity.

ACKNOWLEDGEMENTS

MM acknowledges financial support by a project 'ReSoft' (SEN-13/2015) from the Research Council of Lithuania. We are grateful to Andrew Clayton for discussions on protein production in cells, to Andrei Rode and Eugene Gamaly for continuous search of new phenomena in light–matter interactions and to Etienne Brasselet for joint work on optical vortex generators. VM appreciates support by JSPS Kakenhi Grant No. 15K04637. Partial support via ARC Discovery DP120102980 is acknowledged. SJ is thankful to Gintas Šlekys for the partnership project with Altechna Ltd on industrial fs-laser fabrication.

1 Davis KM, Miura K, Sugimoto N, Hirao K. Writing waveguides in glass with a femtosecond laser. *Opt Lett* 1996; **21**: 1729–1731.
2 Maruo S, Nakamura O, Kawata S. Three-dimensional microfabrication with two-photon-absorbed photopolymerization. *Opt Lett* 1997; **22**: 132–134.
3 Kawata S, Sun HB, Tanaka T, Takada K. Finer features for functional microdevices. *Nature* 2001; **412**: 697–698.
4 Glezer EN, Milosavljevic M, Huang L, Finlay RJ, Her TH *et al.* Three-dimensional optical storage inside transparent materials. *Opt Lett* 1996; **21**: 2023–2025.
5 Watanabe M, Sun HB, Juodkazis S, Takahashi T, Matsuo S *et al.* Three-dimensional optical data storage in vitreous silica. *Jpn J Appl Phys* 1998; **37**: L1527–L1530.
6 Marshall GD, Politi A, Matthews JCF, Dekker P, Ams M *et al.* Laser written waveguide photonic quantum circuits. *Opt Express* 2009; **17**: 12546–12554.
7 Sansoni L, Sciarrino F, Vallone G, Mataloni P, Crespi A *et al.* Polarization entangled state measurement on a chip. *Phys Rev Lett* 2010; **105**: 200503.
8 Deubel M, von Freymann G, Wegener M, Pereira S, Busch K *et al.* Direct laser writing of three-dimensional photonic-crystal templates for telecommunications. *Nat Mater* 2004; **3**: 444–447.
9 Bückmann T, Thiel M, Kadic M, Schittny R, Wegener M. An elasto-mechanical unfeelability cloak made of pentamode metamaterials. *Nat Commun* 2013; **5**: 4130.
10 Wu D, Xu J, Niu LG, Wu SZ, Midorikawa K *et al.* In-channel integration of designable microoptical devices using flat scaffold-supported femtosecond-laser microfabrication for coupling-free optofluidic cell counting. *Light: Sci Appl* 2015; **4**: e228.
11 Malinauskas M, Farsari M, Piskarskas A, Juodkazis S. Ultrafast laser nanostructuring of photopolymers: A decade of advances. *Phys Rep* 2013; **533**: 1–31.
12 Cary HB, Helzer SC. *Modern Welding Technology.* 6th ed. Upper Saddle River, NJ: Pearson Education; 2005.
13 Malinauskas M, Lukosevicius L, Butkus S, Paipulas D. Femtosecond pulse light filament-assisted microfabrication of biodegradable polylactic acid (PLA) material. *J Laser Micro Nanoeng* 2015; **10**: 222–228.
14 Mikutis M, Kudrius T, Slekys G, Paipulas D, Juodkazis S. High 90% efficiency Bragg gratings formed in fused silica by femtosecond Gauss–Bessel laser beams. *Opt Mat Express* 2013; **3**: 1862–1871.
15 Lapointe J, Gagné M, Li MJ, Kashyap R. Making smart phones smarter with photonics. *Opt Express* 2014; **22**: 15473–15483.
16 Minardi S, Milián C, Majus D, Gopal A, Tamosauskas G *et al.* Energy deposition dynamics of femtosecond pulses in water. *Appl Phys Lett* 2014; **105**: 224104.
17 Butkus S, Gaizauskas E, Paipulas D, Viburys Z, Kaskelyte D *et al.* Rapid micro-fabrication of transparent materials using filamented femtosecond laser pulses. *Appl Phys A* 2014; **114**: 81–90.
18 Malinauskas M, Rekstyte S, Lukosevicius L, Butkus S, Balciunas E *et al.* 3D microporous scaffolds manufactured via combination of fused filament fabrication and direct laser writing ablation. *Micromachines* 2014; **5**: 839–858.
19 Matsumoto H, Unrath M, Zhang HB, Hainsey B. Laser direct ablation for patterning printed wiring boards using ultra-fast lasers and high speed beam delivery architectures. *J Laser Micro Nanoeng* 2013; **8**: 315–320.
20 Kato JI, Takeyasu N, Adachi Y, Sun HB, Kawata S. Multiple-spot parallel processing for laser micronanofabrication. *Appl Phys Lett* 2005; **86**: 044102.
21 Stankevicius E, Gertus T, Rutkauskas M, Gedvilas M, Raciukaitis G *et al.* Fabrication of micro-tube arrays in photopolymer SZ2080 by using three different methods of a direct laser polymerization technique. *J Micromech Microeng* 2012; **22**: 065022.
22 Gittard SD, Nguyen A, Obata K, Koroleva A, Narayan RJ *et al.* Fabrication of microscale medical devices by two-photon polymerization with multiple foci via a spatial light modulator. *Biomed Opt Express* 2011; **2**: 3167–3178.
23 Ajeti V, Lien CH, Chen SJ, Su PJ, Squirrell JM *et al.* Image-inspired 3D multiphoton excited fabrication of extracellular matrix structures by modulated raster scanning. *Opt Express* 2013; **21**: 25346–25355.
24 Shank CV, Yen R, Hirlimann C. Time-resolved reflectivity measurements of femtosecond-optical-pulse-induced phase transitions in silicon. *Phys Rev Lett* 1983; **50**: 454–457.
25 Gattass RR, Mazur E. Femtosecond laser micromachining in transparent materials. *Nat Photon* 2008; **2**: 219–225.
26 Sugioka K, Cheng Y. Ultrafast lasers—reliable tools for advanced materials processing. *Light: Sci Appl* 2014; **3**: e149.
27 Marrian CRK, Tennant DM. Nanofabrication. *J Vac Sci Technol A* 2003; **21**: S207–S215.
28 Rekstyte S, Malinauskas M, Juodkazis S. Three-dimensional laser micro-sculpturing of silicone: towards bio-compatible scaffolds. *Opt Express* 2013; **21**: 17028–17041.
29 Buividas R, Mikutis M, Juodkazis S. Surface and bulk structuring of materials by ripples with long and short laser pulses: recent advances. *Prog Quant Electronics* 2014; **38**: 119–156.
30 Phillips R, Kondev J, Theriot J, Garcia H. *Physical Biology of the Cell,* 2nd ed. GS Garland Science; 2012.
31 Iwai H. Roadmap for 22 nm and beyond (invited paper). *Microelectr Eng* 2009; **86**: 1520–1528.
32 Petrochenko PE, Torgersen J, Gruber P, Hicks LA, Zheng JW *et al.* Laser 3D printing with sub-microscale resolution of porous elastomeric scaffolds for supporting human bone stem cells. *Adv Healthc Mater* 2015; **4**: 739–747.
33 Ovsianikov A, Xiao SZ, Farsari M, Vamvakaki M, Fotakis C *et al.* Shrinkage of microstructures produced by two-photon polymerization of Zr-based hybrid photosensitive materials. *Opt Express* 2009; **17**: 2143–2148.

34 Maruo S, Hasegawa T, Yoshimura N. Single-anchor support and supercritical CO_2 drying enable high-precision microfabrication of three-dimensional structures. *Opt Express* 2009; **17**: 20945–20951.
35 Borisov RA, Dorojkina GN, Koroteev NI, Kozenkov VM, Magnitskii SA *et al.* Femtosecond two-photon photopolymerization: a method to fabricate optical photonic crystals with controllable parameters. *Laser Phys* 1998; **8**: 1105–1108.
36 Baldacchini T, LaFratta CN, Farrer RA, Teich MC, Saleh BEA *et al.* Acrylic-based resin with favorable properties for three-dimensional two-photon polymerization. *J Appl Phys* 2004; **95**: 6072–6076.
37 Nguyen LH, Straub M, Gu M. Acrylate-based photopolymer for two-photon microfabrication and photonic applications. *Adv Func Mat* 2005; **15**: 209–216.
38 Serbin J, Ovsianikov A, Chichkov B. Fabrication of woodpile structures by two-photon polymerization and investigation of their optical properties. *Opt Express* 2004; **12**: 5221–5228.
39 Teh WH, Dürig U, Salis G, Harbers R, Drechsler U *et al.* SU-8 for real three-dimensional subdiffraction-limit two-photon microfabrication. *Appl Phys Lett* 2004; **84**: 4095–4097.
40 Juodkazis S, Mizeikis V, Seet KK, Miwa M, Misawa H. Two-photon lithography of nanorods in SU-8 photoresist. *Nanotechnology* 2005; **16**: 846–849.
41 Juodkazis S, Mizeikis V, Misawa H. Three-dimensional microfabrication of materials by femtosecond lasers for photonics applications. *J Appl Phys* 2009; **106**: 051101.
42 von Freymann G, Ledermann A, Thiel M, Staude I, Essig S *et al.* Three-dimensional nanostructures for photonics. *Adv Func Mat* 2010; **20**: 1038–1052.
43 Farsari M, Vamvakaki M, Chichkov BN. Multiphoton polymerization of hybrid materials. *J Opt* 2010; **12**: 124001.
44 Ovsianikov A, Viert J, Chichkov B, Oubaha M, MacCraith B *et al.* Ultra-low shrinkage hybrid photosensitive material for two-photon polymerization microfabrication. *ACS Nano* 2008; **2**: 2257–2262.
45 Terzaki K, Vasilantonakis N, Gaidukeviciute A, Reinhardt C, Fotakis C *et al.* 3D conducting nanostructures fabricated using direct laser writing. *Opt Mater Express* 2011; **1**: 586–597.
46 Sakellari I, Kabouraki E, Gray D, Purlys V, Fotakis C *et al.* Diffusion-assisted high-resolution direct femtosecond laser writing. *ACS Nano* 2012; **6**: 2302–2311.
47 Terzaki K, Kissamitaki M, Skarmoutsou A, Fotakis C, Charitidis CA *et al.* Pre-osteoblastic cell response on three-dimensional, organic-inorganic hybrid material scaffolds for bone tissue engineering. *J Biomed Mat Res A* 2013; **101A**: 2283–2294.
48 Zukauskas A, Bataviciute G, Sciuka M, Balevicius Z, Melninkaitis A *et al.* Effect of the photoinitiator presence and exposure conditions on laser-induced damage threshold of ORMOSIL (SZ2080). *Opt Mat* 2015; **39**: 224–231.
49 Nanoscribe GmbH 2015. Available from http://www.nanoscribe.de/ (updated 5 November 2015).
50 Bückmann T, Stenger N, Kadic M, Kaschke J, Frölich A *et al.* Tailored 3D mechanical metamaterials made by dip-in direct-laser-writing optical lithography. *Adv Mater* 2012; **24**: 2710–2714.
51 Sun HB, Suwa T, Takada K, Zaccaria P, Kim MS *et al.* Shape precompensation in two-photon laser nanowriting of photonic lattices. *Appl Phys Lett* 2004; **85**: 3708–3710.
52 Li Y, Qi FJ, Yang H, Gong QH, Dong XZ *et al.* Nonuniform shrinkage and stretching of polymerized nanostructures fabricated by two-photon photopolymerization. *Nanotechnology* 2008; **19**: 055303.
53 Sun Q, Juodkazis S, Murazawa N, Mizeikis V, Misawa H. Freestanding and movable photonic microstructures fabricated by photopolymerization with femtosecond laser pulses. *J Micromech Microeng* 2010; **20**: 35004–35008.
54 Zhou WH, Kuebler SM, Braun KL, Yu TY, Cammack JK *et al.* An efficient two-photon-generated photoacid applied to positive-tone 3D microfabrication. *Science* 2002; **296**: 1106–1109.
55 Gansel JK, Thiel M, Rill MS, Decker M, Bade K *et al.* Gold helix photonic metamaterial as broadband circular polarizer. *Science* 2009; **325**: 1513–1515.
56 Malinauskas M, Zukauskas A, Bickauskaite G, Gadonas R, Juodkazis S. Mechanisms of three-dimensional structuring of photo-polymers by tightly focussed femtosecond laser pulses. *Opt Express* 2010; **18**: 10209–10221.
57 Maruo S, Ikuta K. Three-dimensional microfabrication by use of single-photon-absorbed polymerization. *Appl Phys Lett* 2000; **76**: 2656–2658.
58 Seet KK, Juodkazis S, Jarutis V, Misawa H. Feature-size reduction of photopolymerized structures by femtosecond optical curing of SU-8. *Appl Phys Lett* 2006; **89**: 024106.
59 Brasselet E, Malinauskas M, Zukauskas A, Juodkazis S. Photopolymerized microscopic vortex beam generators: precise delivery of optical orbital angular momentum. *Appl Phys Lett* 2010; **97**: 211108.
60 Mizeikis V, Seet KK, Juodkazis S, Misawa H. Three-dimensional woodpile photonic crystal templates for the infrared spectral range. *Opt Lett* 2004; **29**: 2061–2063.
61 Seet KK, Mizeikis V, Juodkazis S, Misawa H. Three-dimensional horizontal circular spiral photonic crystals with stop gaps below 1 μm. *Appl Phys Lett* 2006; **88**: 221101.
62 Sun HB, Takada K, Kawata S. Elastic force analysis of functional polymer submicron oscillators. *Appl Phys Lett* 2001; **79**: 3173–3175.
63 Park SH, Yang DY, Lee KS. Two-photon stereolithography for realizing ultraprecise three-dimensional nano/microdevices. *Laser Photon Rev* 2009; **3**: 1–11.
64 Farsari M, Chichkov BN. Materials processing: Two-photon fabrication. *Nat Photon* 2009; **3**: 450–452.
65 Zhang YL, Chen QD, Xia H, Sun HB. Designable 3D nanofabrication by femtosecond laser direct writing. *NanoToday* 2010; **5**: 435–448.
66 He F, Liao Y, Lin J, Song J, Qiao L *et al.* Femtosecond laser fabrication of monolithically integrated micfrofluidic sensors in glass. *Sensors* 2014; **14**: 19402–19440.
67 Hohmann JK, Renner M, Waller EH, von Freymann G. Three-dimensional μ-printing: an enabling technology. *Adv Opt Mat* 2015; **3**: 1488–1507.
68 Newport Corp 2016. Available from http://www.newport.com/ (updated 5 November 2015).
69 Altechna R&D, 2015. Available from http://www.wophotonics.com/ (updated 5 November 2015).
70 Photonic Solution Ltd 2015. Available from http://www.photonicsolutions.co.uk/ (updated 5 November 2015).
71 Danilevicius P, Rekstyte S, Balciunas E, Kraniauskas A, Jarasiene R *et al.* Micro-structured polymer scaffolds fabricated by direct laser writing for tissue engineering. *J Biomed Opt* 2012; **17**: 081405.
72 Torgersen J, Qin XH, Li ZQ, Ovsianikov A, Liska R *et al.* Hydrogels for two-photon polymerization: a toolbox for mimicking the extracellular matrix. *Adv Func Mat* 2013; **23**: 4542–4554.
73 Fischer J, Wegener M. Three-dimensional direct laser writing inspired by stimulated-emission-depletion microscopy (invited). *Opt Mat Express* 2011; **1**: 614–624.
74 Waller EH, Renner M, von Freymann G. Active aberration- and point-spread-function control in direct laser writing. *Opt Express* 2012; **20**: 24949–24956.
75 Klar TA, Wollhofen R, Jacak J. Sub-Abbe resolution: from STED microscopy to STED lithography. *Phys Scr* 2014; **2014**: 014049.
76 Tielen V, Bellouard Y. Three-dimensional glass monolithic micro-flexure fabricated by femtosecond laser exposure and chemical etching. *Micromachines* 2014; **5**: 697–710.
77 in't Velda BH, Overmeyer L, Schmidt M, Wegener K, Malshe A *et al.* Micro additive manufacturing using ultra short laser pulses. *CIRP Annal Manufact Technol* 2015; **64**: 701–724.
78 Tan DZ, Sharafudeen KN, Yue YZ, Qiu JR. Femtosecond laser induced phenomena in transparent solid materials: fundamentals and applications. *Prog Mat Sci* 2016; **76**: 154–228.
79 Liberale C, Cojoc G, Candeloro P, Das G, Gentile F *et al.* Micro-optics fabrication on top of optical fibers using two-photon lithography. *IEEE Photon Technol Lett* 2010; **22**: 474–476.
80 Malinauskas M, Zukauskas A, Purlys V, Belazaras K, Momot A *et al.* Femtosecond laser polymerization of hybrid/integrated micro-optical elements and their characterization. *J Opt* 2010; **12**: 124010.
81 Zukauskas A, Melissinaki V, Kaskelyte D, Farsari M, Malinauskas M. Improvement of the fabrication accuracy of fiber tip microoptical components via mode field expansion. *J Laser Micro Nanoeng* 2014; **9**: 68–72.
82 Lin XF, Hu GQ, Chen QD, Niu LG, Li QS *et al.* A light-driven turbine-like micro-rotor and study on its light-to-mechanical power conversion efficiency. *Appl Phys Lett* 2012; **101**: 113901.
83 Malinauskas M, Zukauskas A, Belazaras K, Tikuisis K, Purlys V *et al.* Laser fabrication of various polymer microoptical components. *Eur Phys J Appl Phys* 2012; **58**: 20501.
84 Beresna M, Gecevicius M, Kazansky PG. Polarization sensitive elements fabricated by femtosecond laser nanostructuring of glass (invited). *Opt Mater Express* 2011; **1**: 783–795.
85 Zhang JY, Gecevicius M, Beresna M, Kazansky PG. Seemingly unlimited lifetime data storage in nanostructured glass. *Phys Rev Lett* 2014; **112**: 033901.
86 Xu JJ, Yao WG, Tian ZN, Wang L, Guan KM *et al.* High curvature concave–convex microlens. *IEEE Photon Technol Lett* 2015; **27**: 2465–2468.
87 Wu D, Wang JN, Niu LG, Zhang XL, Wu SZ *et al.* Bioinspired fabrication of high-quality 3D artificial compound eyes by voxel-modulation femtosecond laser writing for distortion-free wide-field-of-view imaging. *Adv Opt Mat* 2014; **2**: 751–758.
88 Tian ZN, Yao WG, Xu JJ, Yu YH, Chen QD *et al.* Focal varying microlens array. *Opt Lett* 2015; **40**: 4222–4225.
89 Jin P, Gao YL, Liu TT, Li XJ, Tan JB. Resist shaping for replication of micro-optical elements with continuous relief in fused silica. *Opt Lett* 2010; **35**: 1169–1171.
90 Gao YL, Lin J, Jin P, Tan JB, Davies G *et al.* Stop grating for perfect replication of micro Fresnel lens by thermal imprinting. *J Micromech Microeng* 2012; **22**: 065018.
91 Schumann M, Buckmann T, Gruhler N, Wegener M, Pernice W. Hybrid 2D–3D optical devices for integrated optics by direct laser writing. *Light: Sci Appl* 2014; **3**: e175.
92 Liu DX, Sun YL, Dong WF, Yang RZ, Chen QD *et al.* Dynamic laser prototyping for biomimetic nanofabrication. *Laser Photon Rev* 2014; **8**: 882–888.
93 Zukauskas A, Matulaitiene I, Paipulas D, Niaura G, Malinauskas M *et al.* Tuning the refractive index in 3D direct laser writing lithography: Towards GRIN microoptics. *Laser Photon Rev* 2015; **9**: 706–712.
94 Mizeikis V, Purlys V, Buividas R, Juodkazis S. Realization of structural color by direct laser write technique in photoresist. *J Laser Micro Nanoeng* 2014; **9**: 42–45.
95 Sun HB, Matsuo S, Misawa H. Three-dimensional photonic crystal structures achieved with two-photon-absorption photopolymerization of resin. *Appl Phys Lett* 1999; **74**: 786–788.
96 Kaneko K, Sun HB, Duan X, Kawata S. Submicron diamond-lattice photonic crystals produced by two-photon laser nanofabrication. *Appl Phys Lett* 2003; **83**: 2091–2093.
97 Serbin J, Gu M. Experimental evidence for superprism effects in three-dimensional polymer photonic crystals. *Adv Mater* 2006; **18**: 221–224.
98 Tétreault N, von Freymann G, Deubel M, Hermatschweiler M, Pérez-Willard F *et al.* New route to three-dimensional photonic bandgap materials: silicon double inversion of polymer templates. *Adv Mater* 2006; **18**: 457–460.

99 Seet KK, Mizeikis V, Kannari K, Juodkazis S, Misawa H *et al.* Templating and replication of spiral photonic crystals for silicon photonics. *IEEE J Select Topics Quant Electr* 2008; **14**: 1064–1073.
100 Vasilantonakis N, Terzaki K, Sakellari I, Purlys V, Gray D *et al.* Three-dimensional metallic photonic crystals with optical bandgaps. *Adv Mater* 2012; **24**: 1101–1105.
101 Maigyte L, Purlys V, Trull J, Peckus M, Cojocaru C *et al.* Flat lensing in the visible frequency range by woodpile photonic crystals. *Opt Lett* 2013; **38**: 2376–2378.
102 Wong S, Deubel M, Pérez-Willard F, John S, Ozin GA *et al.* Direct laser writing of three-dimensional photonic crystals with a complete photonic bandgap in chalcogenide glasses. *Adv Mater* 2006; **18**: 265–269.
103 Seet KK, Mizeikis V, Matsuo S, Juodkazis S, Misawa H. Three-dimensional spiral-architecture photonic crystals obtained by direct laser writing. *Adv Mater* 2005; **17**: 541–545.
104 Thiel M, Decker M, Deubel M, Wegener M, Linden S *et al.* Polarization stop bands in chiral polymeric three-dimensional photonic crystals. *Adv Mater* 2007; **19**: 207–210.
105 Deubel M, Wegener M, Kaso A, John S. Direct laser writing and characterization of "slanted pore" photonic crystals. *Appl Phys Lett* 2004; **85**: 1895–1897.
106 Thiel M, Rill MS, von Freymann G, Wegener M. Three-dimensional bi-chiral photonic crystals. *Adv Mater* 2009; **21**: 4680–4682.
107 Joannopoulos JD, Johnson SG, Winn JN, Meade RD. *Photonic Crystals: Molding the Flow of Light,* 2nd ed. Princeton: Princeton University Press; 2008.
108 Fischer J, von Freymann G, Wegener M. The materials challenge in diffraction-unlimited direct-laser-writing optical lithography. *Adv Mater* 2010; **22**: 3578–3582.
109 Wollhofen R, Katzmann J, Hrelescu C, Jacak J, Klar TA. 120 nm resolution and 55 nm structure size in STED-lithography. *Opt Express* 2013; **21**: 10831–10840.
110 Fischer J, Wegener M. Three-dimensional optical laser lithography beyond the diffraction limit. *Laser Photon Rev* 2013; **7**: 22–44.
111 Thiel M, Ott J, Radké A, Kaschke J, Wegener M. Dip-in depletion optical lithography of three-dimensional chiral polarizers. *Opt Lett* 2013; **38**: 4252–4255.
112 Rittweger E, Han KY, Irvine SE, Eggeling C, Hell SW. STED microscopy reveals crystal colour centres with nanometric resolution. *Nat Photon* 2009; **3**: 144–147.
113 Fischer J, Wegener M. Ultrafast polymerization inhibition by stimulated emission depletion for three-dimensional nanolithography. *Adv Mater* 2012; **24**: OP65–OP69.
114 Fourkas JT. Nanoscale photolithography with visible light. *J Phys Chem Lett* 2010; **1**: 1221–1227.
115 Li LJ, Gattass RR, Gershgoren E, Hwang H, Fourkas JT. Achieving $\lambda/20$ resolution by one-color initiation and deactivation of polymerization. *Science* 2009; **324**: 910–913.
116 Wiesbauer M, Wollhofen R, Vasic B, Schilcher K, Jacak J *et al.* Nano-anchors with single protein capacity produced with STED lithography. *Nano Lett* 2013; **13**: 5672–5678.
117 Mueller JB, Fischer J, Mayer F, Kadic M, Wegener M. Polymerization kinetics in three-dimensional direct laser writing. *Adv Mater* 2014; **26**: 6566–6571.
118 Jiang LJ, Zhou YS, Xiong W, Gao Y, Huang X *et al.* Two-photon polymerization: investigation of chemical and mechanical properties of resins using Raman micro-spectroscopy. *Opt Lett* 2014; **39**: 3034–3037.
119 Mueller P, Thiel M, Wegener M. 3D direct laser writing using a 405 nm diode laser. *Opt Lett* 2014; **39**: 6847–6850.
120 Malinauskas M, Rekstyte S, Jonavicius T, Mizeikis V, Gamaly E *et al.* Femtosecond pulsed light polarization induced peculiarities in direct laser writing 3D nanolithography. *Proc. CLEO* 2015; **CM1**: 2.
121 Lindenmann N, Balthasar G, Hillerkuss D, Schmogrow R, Jordan M *et al.* Photonic wire bonding: a novel concept for chip-scale interconnects. *Opt Express* 2012; **20**: 17667–17677.
122 Lindenmann N, Dottermusch S, Goedecke ML, Hoose T, Billah MR *et al.* Connecting silicon photonic circuits to multicore fibers by photonic wire bonding. *J Lightwave Technol* 2015; **33**: 755–760.
123 Gamaly EG, Rapp L, Roppo V, Juodkazis S, Rode AV. Generation of high energy density by fs-laser induced confined microexplosion. *New J Phys* 2013; **15**: 025018.
124 Gamaly EG, Vailionis A, Mizeikis V, Yang W, Rode AV *et al.* Warm dense matter at the bench-top: Fs-laser induced confined microexplosion. *High Energ Dens Phys* 2012; **8**: 13–17.
125 Bressel L, de Ligny D, Sonneville C, Martinez V, Mizeikis V *et al.* Femtosecond laser induced density changes in GeO_2 and SiO_2 glasses: fictive temperature effect. *Opt Mater Express* 2011; **1**: 605–613.
126 Buividas R, Gervinskas G, Tadich A, Cowie BCC, Mizeikis V *et al.* Phase transformation in laser-induced micro-explosion in olivine $(Fe,Mg)_2SiO_4$. *Adv Eng Mater* 2014; **16**: 767–773.
127 Juodkazis S, Nishimura K, Misawa H, Ebisui T, Waki R *et al.* Control over the crystalline state of sapphire. *Adv Mater* 2006; **18**: 1361–1364.
128 Vailionis A, Gamaly EG, Mizeikis V, Yang WG, Rode AV *et al.* Evidence of super-dense aluminium synthesized by ultra-fast micro-explosion. *Nat Commun* 2011; **2**: 445.
129 Juodkazis S, Misawa H, Gamaly EG, Luther-Davis B, Hallo L *et al.* Is the nano-explosion really microscopic? *J Non-Crystall Solids* 2009; **355**: 1160–1162.
130 Watanabe M, Juodkazis S, Sun HB, Matsuo S, Misawa H. Luminescence and defect formation by visible and near-infrared irradiation of vitreous silica. *Phys Rev B* 1999; **60**: 9959–9964.
131 Sun HB, Juodkazis S, Watanabe M, Matsuo S, Misawa H *et al.* Generation and recombination of defects in vitreous silica induced by irradiation with a near-infrared femtosecond laser. *J Phys Chem B* 2000; **104**: 3450–3455.
132 Kudrius T, Slekys G, Juodkazis S. Surface-texturing of sapphire by femtosecond laser pulses for photonic applications. *J Phys D: Appl Phys* 2010; **43**: 145501.
133 Marcinkevicius A, Juodkazis S, Watanabe M, Miwa M, Matsuo S *et al.* Femtosecond laser-assisted three-dimensional microfabrication in silica. *Opt Lett* 2001; **26**: 277–279.
134 Juodkazis S, Misawa H, Hashimoto T, Gamaly EG, Luther-Davies B. Laser-induced micro-explosion confined in a bulk of silica: formation of nanovoids. *Appl Phys Lett* 2006; **88**: 201909.
135 Juodkazis S, Nishi Y, Misawa H. Femtosecond laser-assisted formation of channels in sapphire using KOH solution. *RRL-Phys Stat Sol* 2008; **2**: 275–277.
136 Vitek DN, Block E, Bellouard Y, Adams DE, Backus S *et al.* Spatio-temporally focused femtosecond laser pulses for nonreciprocal writing in optically transparent materials. *Opt Express* 2010; **18**: 24673–24678.
137 Kazansky PG, Shimotsuma Y, Sakakura M, Beresna M, Gecevicius M *et al.* Photosensitivity control of an isotropic medium through polarization of light pulses with tilted intensity front. *Opt Express* 2011; **19**: 20657–20664.
138 Juodkazis S, Nishimura K, Misawa H. Three-dimensional laser structuring of materials at tight focusing. *Chin Opt Lett* 2007; **5**: S198–S200.
139 Hatanaka K, Ida T, Ono H, Matsushima SI, Fukumura H *et al.* Chirp effect in hard X-ray generation from liquid target when irradiated by femtosecond pulses. *Opt Express* 2008; **16**: 12650–12657.
140 Richter S, Nolte S, Tünnermann A. Ultrashort pulse laser welding—a new approach for high-stability bonding of different glasses. *Phys Proceed* 2012; **39**: 556–562.
141 Sano T, Iwasaki S, Ozeki Y, Itoh K, Hirose A. Femtosecond laser direct joining of copper with polyethylene terephthalate. *Mater Trans* 2013; **54**: 926–930.
142 Kabashin AV, Meunier M. Synthesis of colloidal nanoparticles during femtosecond laser ablation of gold in water. *J Appl Phys* 2003; **94**: 7941–7943.
143 Kubiliute R, Maximova KA, Lajevardipour A, Yong J, Hartley JS *et al.* Ultra-pure, water-dispersed Au nanoparticles produced by femtosecond laser ablation and fragmentation. *Int J Nanomed* 2013; **8**: 2601–2611.
144 Morikawa J, Orie A, Hashimoto T, Juodkazis S. Thermal and optical properties of the femtosecond-laser-structured and stress-induced birefringent regions in sapphire. *Opt Express* 2010; **18**: 8300–8310.
145 Chen F, de Aldana JRV. Optical waveguides in crystalline dielectric materials produced by femtosecond-laser micromachining. *Laser Photon Rev* 2014; **8**: 251–275.
146 Thomson RR, Birks TA, Leon-Saval SG, Kar AK, Bland-Hawthorn J. Ultrafast laser inscription of an integrated photonic lantern. *Opt Express* 2011; **19**: 5698–5705.
147 Jovanovic N, Spaleniak I, Gross S, Ireland M, Lawrence JS *et al.* Integrated photonic building blocks for next-generation astronomical instrumentation I: the multimode waveguide. *Opt Express* 2012; **20**: 17029–17043.
148 Spaleniak I, Gross S, Jovanovic N, Williams RJ, Lawrence JS *et al.* Multiband processing of multimode light: combining 3D photonic lanterns with waveguide Bragg gratings. *Laser Photon Rev* 2014; **8**: L1–L5.
149 Spaleniak I, Jovanovic N, Gross S, Ireland MJ, Lawrence JS *et al.* Integrated photonic building blocks for next-generation astronomical instrumentation II: the multimode to single mode transition. *Opt Express* 2013; **21**: 27197–27208.
150 Bland-Hawthorn J, Kern P. Astrophotonics: a new era for astronomical instruments. *Opt Express* 2009; **17**: 1880–1884.
151 Ams M, Marshall GD, Dekker P, Piper JA, Withford MJ. Ultrafast laser written active devices. *Laser Photon Rev* 2009; **3**: 535–544.
152 Haque M, Lee KKC, Ho S, Fernandes LA, Herman PR. Chemical-assisted femtosecond laser writing of lab-in-fibers. *Lab Chip* 2014; **14**: 3817–3829.
153 Birks TA, Gris-Sánchez I, Yerolatsitis S, Leon-Saval SG, Thomson RR. The photonic lantern. *Adv Opt Photon* 2015; **7**: 107–167.
154 Maciulaitis J, Deveikyte M, Rekstyte S, Bratchikov M, Darinskas A *et al.* Preclinical study of SZ2080 material 3D microstructured scaffolds for cartilage tissue engineering made by femtosecond direct laser writing lithography. *Biofabrication* 2015; **7**: 015015.
155 Christensen CM. *The Innovator's Dilemma: When New Technologies Cause Great Firms to Fail.* Boston, MA: Harvard Business School Press; 1997.
156 Poh PSP, Hutmacher DW, Stevens MM, Woodruff MA. Fabrication and *in vitro* characterization of bioactive glass composite scaffolds for bone regeneration. *Biofabrication* 2013; **5**: 045005.
157 Ovsianikov A, Mühleder S, Torgersen J, Li ZQ, Qin XH *et al.* Laser photofabrication of cell-containing hydrogel constructs. *Langmuir* 2014; **30**: 3787–3794.
158 Marino A, Filippeschi C, Mattoli V, Mazzolai B, Ciofani G. Biomimicry at the nanoscale: current research and perspectives of two-photon polymerization. *Nanoscale* 2015; **7**: 2841–2850.
159 Juodkazis S, Mizeikis V, Seet KK, Misawa H, Wegst UGK. Mechanical properties and tuning of three-dimensional polymeric photonic crystals. *Appl Phys Lett* 2007; **91**: 241904.
160 Klein F, Richter B, Striebel T, Franz CM, von Freymann G *et al.* Two-component polymer scaffolds for controlled three-dimensional cell culture. *Adv Mater* 2011; **23**: 1341–1345.
161 Rekstyte S, Kaziulionyte E, Balciunas E, Kaskelyte D, Malinauskas M. Direct laser fabrication of composite material 3D microstructured scaffolds. *J Laser Micro/Nanoeng* 2014; **9**: 25–30.
162 Clayton AHA. Cell surface receptors in the 21st century. *AIMS Biophys* 2014; **1**: 51–52.
163 Bauer J, Hengsbach S, Tesari I, Schwaiger R, Kraft O. High-strength cellular ceramic composites with 3D microarchitecture. *Proc Natl Sci USA* 2014; **111**: 2453–2458.
164 Sun YL, Li Q, Sun SM, Huang JC, Zheng BY *et al.* Aqueous multiphoton lithography with multi-functional silk-centered bio-resists. *Nat Commun* 2015; **6**: 8612.
165 Piqué A, Kim H. Laser-induced forward transfer of functional materials: advances and future directions. *J Laser Micro Nanoeng* 2014; **9**: 192–197.

166 Hallo L, Mézel C, Bourgeade A, Hébert D, Gamaly EG *et al*. Laser-matter interaction in transparent materials: confined micro-explosion and jet formation. In: Hall TJ, Gaponenko SV, Paredes SA editors. *Extreme Photonics & Applications*. Netherlands: Springer; 2010, pp 121–146.
167 Danieliene E, Gabryte E, Danielius R, Vengris M, Vaiceliunaite A *et al*. Corneal stromal ablation with femtosecond ultraviolet pulses in rabbits. *J Cataract Refract Surg* 2012; **39**: 258–267.
168 Kim D, So PTC. High-throughput three-dimensional lithographic microfabrication. *Opt Lett* 2010; **35**: 1602–1604.
169 Hasegawa S, Hayasaki Y. Holographic vector wave femtosecond laser processing. *Int J Optomechatr* 2014; **8**: 73–88.
170 Tumbleston JR, Shirvanyants D, Ermoshkin N, Janusziewicz R, Johnson AR *et al*. Continuous liquid interface production of 3D objects. *Science* 2015; **347**: 1349–1352.
171 Obata K, Koch J, Hinze U, Chichkov BN. Multi-focus two-photon polymerization technique based on individually controlled phase modulation. *Opt Express* 2010; **18**: 17193–17200.
172 Waller EH, von Freymann G. Multi foci with diffraction limited resolution. *Opt Express* 2013; **21**: 21708–21713.
173 Vizsnyiczai G, Kelemen L, Ormos P. Holographic multi-focus 3D two-photon polymerization with real-time calculated holograms. *Opt Express* 2014; **22**: 24217–24223.
174 Gecevicius M, Beresna M, Drevinskas R, Kazansky PG. Airy beams generated by ultrafast laser-imprinted space-variant nanostructures in glass. *Opt Lett* 2014; **39**: 6791–6794.
175 Bonse J, Baudach S, Krüger J, Kautek W, Lenzner M. Femtosecond laser ablation of silicon-modification thresholds and morphology. *Appl Phys A* 2002; **74**: 19–25.
176 Gedvilas M, Miksys J, Raciukaitis G. Flexible periodical micro- and nano-structuring of a stainless steel surface using dual-wavelength double-pulse picosecond laser irradiation. *RSC Adv* 2015; **5**: 75075–75080.
177 Cumming BP, Jesacher A, Booth MJ, Wilson T, Gu M. Adaptive aberration compensation for three-dimensional micro-fabrication of photonic crystals in lithium niobate. *Opt Express* 2011; **19**: 9419–9425.
178 Marcinkevicius A, Mizeikis V, Juodkazis S, Matsuo S, Misawa H. Effect of refractive index-mismatch on laser microfabrication in silica glass. *Appl Phys A* 2003; **76**: 257–260.
179 Rogel-Salazar J, Jiménez-Romero HA, Chávez-Cerda S. Full characterization of Airy beams under physical principles. *Phys Rev A* 2014; **89**: 023807.
180 Marcinkevicius A, Juodkazis S, Matsuo S, Mizeikis V, Misawa H. Application of Bessel beams for microfabrication of dielectrics by femtosecond laser. *Jpn J Appl Phys* 2001; **40**: L1197–L1199.
181 Sheppard CJR, Wilson T. Gaussian-beam theory of lenses with annular aperture. *IEEE J Microwaves Opt Acoust* 1978; **2**: 105–112.
182 Durnin J, Miceli JJ, Eberly JH. Diffraction-free beams. *Phys Rev Lett* 1987; **58**: 1499–1501.
183 Hasegawa S, Hayasaki Y. Adaptive optimization of a hologram in holographic femtosecond laser processing system. *Opt Lett* 2009; **34**: 22–24.
184 Sun YL, Dong WF, Niu LG, Jiang T, Liu DX *et al*. Protein-based soft micro-optics fabricated by femtosecond laser direct writing. *Light: Sci Appl* 2014; **3**: e129.
185 Gladwell M. *The Tipping Point: How Little Things Can Make a Big Difference*. New York: Back Bay Books; 2000.

This work is licensed under a Creative Commons Attribution 4.0 International License. The images or other third party material in this article are included in the article's Creative Commons license, unless indicated otherwise in the credit line; if the material is not included under the Creative Commons license, users will need to obtain permission from the license holder to reproduce the material. To view a copy of this license, visit http://creativecommons.org/licenses/by/4.0/